



*Dedicated to the memory of  
Dr. Henry V. Kehiaian (1929–2009)*

## PHASE FORMATION MECHANISM IN THE ZnO-SnO<sub>2</sub> BINARY SYSTEM

Susana MIHAIU\*, Irina ATKINSON, Oana MOCIOIU, Alexandra TOADER, Ecaterina TENEA  
and Maria ZAHARESCU

“Ilie Murgulescu” Institute of Physical Chemistry of the Roumanian Academy, 202 Spl. Independentei, 060021 Bucharest, Roumania

Received July 8, 2010

The Sn-Zn-O ceramics are very interesting materials for their applications as varistors, electrodes, catalysts and gas sensors. The present work deals with phase formations studies in the SnO<sub>2</sub>-ZnO binary system over the whole concentration range. High-temperature interactions of the samples thermally treated in the 1000-1500°C domain were evaluated by XRD and FT-IR Spectroscopy. Besides SnO<sub>2</sub> and ZnO only Zn<sub>2</sub>SnO<sub>4</sub> ternary compound was found in our experimental conditions.

### INTRODUCTION

The interest for ZnO and SnO<sub>2</sub> oxides is very high due to their specific semiconducting properties that make them suitable for different applications, as varistors,<sup>1</sup> thermoelectric materials with high-energy conversion efficiency,<sup>2</sup> gas sensors.<sup>3</sup> Nowadays, commercial ZnO-based varistors are produced with minor additions of typically Bi<sub>2</sub>O<sub>3</sub>, Sb<sub>2</sub>O<sub>3</sub>, CoO, MnO<sub>2</sub> and Cr<sub>2</sub>O<sub>3</sub>.<sup>4</sup> Gas sensing property of SnO<sub>2</sub>-based ceramics was improved by addition of different additives,<sup>5</sup> while modified SnO<sub>2</sub> anodes have been used for the degradation of phenolic compounds<sup>6</sup> or in electrowinning processes.<sup>7</sup>

Literature data reported the formation of two compounds in the ZnO-SnO<sub>2</sub> system, namely zinc orthostannate with formula Zn<sub>2</sub>SnO<sub>4</sub> and zinc metastannate, ZnSnO<sub>3</sub>, respectively.

Mixtures of ZnO and SnO<sub>2</sub> powders with 2:1 molar ratio exhibit photocatalytic performance for methyl orange degradation.<sup>8</sup> Ceramic varistors with extensive regions of Zn<sub>2</sub>SnO<sub>4</sub> have been obtained by Anastasiou *et al.*<sup>9</sup>

Literature data indicate that the formation temperature of the Zn<sub>2</sub>SnO<sub>4</sub> compound strongly depends on the preparation method.<sup>8,10-12</sup>

The formation of ZnSnO<sub>3</sub> is still ambiguous and contradictory. Shen and Zhang<sup>13</sup> reported a pure ZnSnO<sub>3</sub> phase with a perovskite-type structure which can be obtained only by a co-precipitation method using together oxalic acid and ammonia as precipitants. Kovacheva and Petrov<sup>14</sup> however showed that ZnSnO<sub>3</sub> can not adopt a perovskite structure under normal conditions, since the ionic radius of Zn<sup>2+</sup> is too small. They succeeded to prepare ZnSnO<sub>3</sub> with an ilmenite-type structure by an ion-exchange reaction between Li<sub>2</sub>SnO<sub>3</sub> and a melt of ZnCl<sub>2</sub>-KCl. New type of ZnSnO<sub>3</sub> based varistor was obtained by Zang *et al.*<sup>15</sup> at 1427°C, in pressed pellets at 160 MP. Zinc metastannate exhibits a limited thermal stability and in bulk samples its decomposition to Zn<sub>2</sub>SnO<sub>4</sub> and SnO<sub>2</sub> has been noted at temperatures as low as 600 °C.<sup>16</sup> A polar ZnSnO<sub>3</sub> oxide with a LiNbO<sub>3</sub>-type structure (LN) was synthesized by solid state reaction at 1000 °C under a pressure of 7 GPa<sup>17</sup> and the authors affirm that ZnSnO<sub>3</sub> is stable up to 700 °C.

\* Corresponding author: smihaiu@icf.ro

Based on the serious discrepancies, that can still be found in the literature regarding the thermal evolution of the ZnO–SnO<sub>2</sub> binary system; in the present work a systematic study of the phase formation over the whole compositional range of the ZnO–SnO<sub>2</sub> binary system in the 500–1500 °C temperature domain was approached.

## EXPERIMENTAL

Mixtures of SnO<sub>2</sub> (Merck - reagent grade) and ZnO (Merck - reagent grade) powders with grain size up to 60 µm were wet homogenized during 15 minutes in the agate mortar in absolute ethanol. Initial molar compositions of the oxide mixtures, labeled 1-16 SZO, are shown in the Table 1.

Cylindrical samples with  $\Phi=10$  mm and  $h=2-3$  mm were obtained by pressing at 100 MPa. The sample of (1-16) SZO, were calcined in a Nabertherm type oven at 500, 600, 800, 850, 900 and 1000°C for 10 hours. The CARBOLITE HTF 1700 furnace was used for thermal treatment at higher temperatures, namely, at 1100, 1150, 1200, 1300, 1500°C. After thermal treatment, all samples were cooled to room temperature with the furnace.

DTA and TG/DTG investigations were performed with a Mettler Toledo Derivatograph in the 20–1500°C temperature range with a heating rate of 5°C/min.

X-ray analysis of the obtained calcined samples was performed using a Rigaku Ultima IV diffractometer with Cu K $\alpha$  radiation, with the scan step of 0.02° and scan speed of 5°/min. For XRD analyses following PDF Cards were used: SnO<sub>2</sub> 01-071-0652; ZnO 00-036-1451; Zn<sub>2</sub>SnO<sub>4</sub> 00-024-1470; ZnSnO<sub>3</sub> 01-089-0095.

Room temperature infrared transmission measurements (FT-IR spectra) on the thermally treated samples were made with a Nicolet 6700 apparatus in 400–4000 cm<sup>-1</sup> range. The spectra were taken from thin transparent (~20 mg/cm<sup>2</sup>) KBr pellets containing approximately 0.5% wt samples. Pellets were

prepared by compacting and vacuum-pressing an intimate mixture obtained by grinding 1 mg of substance in 200 mg KBr.

The microstructure of the samples was observed by Scanning Electron Microscopy (SEM FEI Quanta 200 type).

## RESULTS

### 1. Phase formation in non-isothermal conditions

X-Ray diffractions patterns of SnO<sub>2</sub> and ZnO starting oxides are presented in Fig. 1. In the case of SnO<sub>2</sub> its rutile structure is confirmed (PDF Card: 01-071-0652) while in the case of ZnO the wurtzite structure was identified (PDF Card: 00-036-1451).

In order to establish the high temperature interaction in the ZnO–SnO<sub>2</sub> binary mixtures, in non-isothermal conditions, the thermal analysis curves have been recorded up to 1500°C for the following samples: 1SZO (pure SnO<sub>2</sub>), 8SZO (with SnO<sub>2</sub>:ZnO=1:1 molar ratio), 10SZO (with SnO<sub>2</sub>:ZnO=1:2 molar ratio) and 16SZO (pure ZnO). No thermal effects were observed on the DTA curves of the investigated samples indicating a continuously occurring interaction between the two components and not one at a given temperature represented by a definite thermal effect.

In Fig. 2 the XRD pattern of DTA residue of 8SZO sample is presented, showing the presence of the diffraction lines corresponding to a mixture of Zn<sub>2</sub>SnO<sub>4</sub> and SnO<sub>2</sub>. The obtained result indicates that in non-isothermal conditions the formation of ZnSnO<sub>3</sub> did not occur.

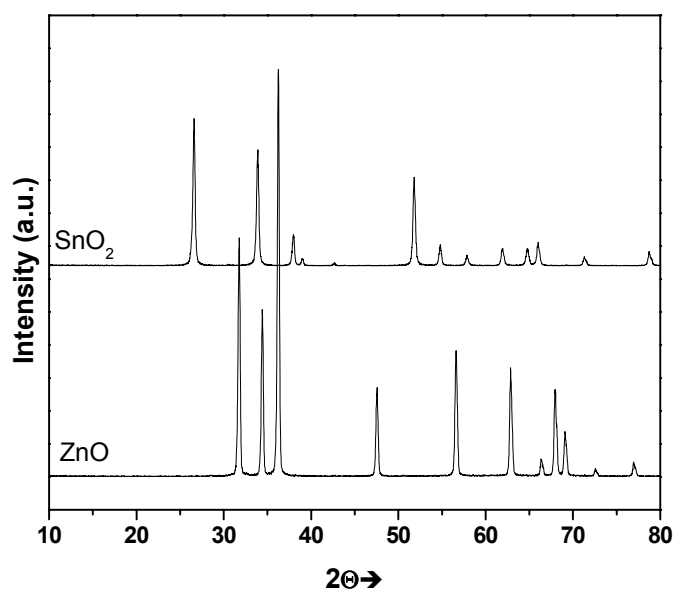


Fig. 1 – XRD patterns of the starting oxides.

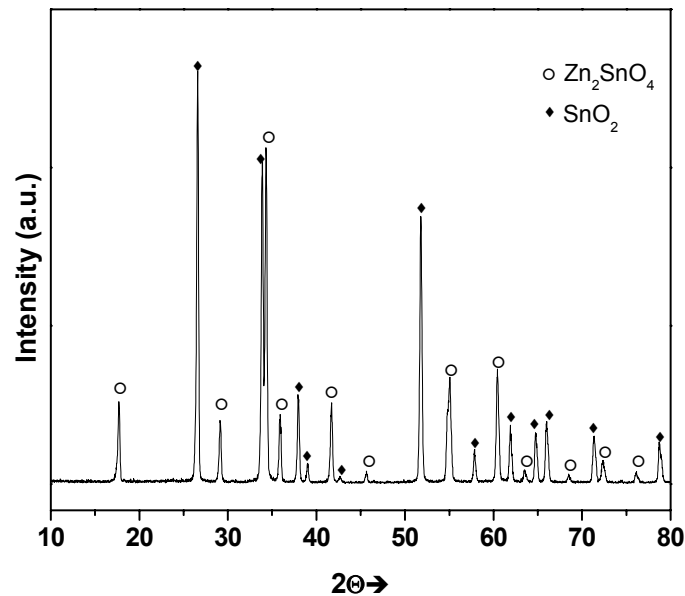


Fig. 2 – XRD pattern of DTA residue for 8SZO sample.

## 2. Phase formation in isothermal conditions

Considering literature data regarding the formation of different phases of interest in the studied system and based on the results obtained in non-isothermal conditions, all prepared samples (labeled 1-16 SZO) were thermally treated for ten hours at 500, 600, 800, 850, 900, 1000, 1100, 1150, 1300, 1400 and 1500 °C temperatures, as mentioned above.

In Table 1 initial composition and phase composition at representative temperatures of thermal treatment for all samples are shown, while in Figs. 3 and 4 XRD patterns for some selected samples thermally treated at 1300 °C are presented.

Up to 900 °C only tetragonal SnO<sub>2</sub> and trigonal ZnO phases were identified by XRD analysis.

At 900 °C for the 4-12 SZO samples, beside SnO<sub>2</sub> and ZnO, the presence of Zn<sub>2</sub>SnO<sub>4</sub> inverse spinel was emphasized.

At temperatures ≥ 1000 °C for the sample 10SZO (with SnO<sub>2</sub>/ZnO=1:2 molar ratio) the pure

spinel Zn<sub>2</sub>SnO<sub>4</sub> phase was identified. In the case of 8SZO sample (with SnO<sub>2</sub>/ZnO=1:1 molar ratio), in the same temperature range the formation of corresponding ZnSnO<sub>3</sub> was not identified, but the XRD characteristic lines of the mixture of SnO<sub>2</sub> and Zn<sub>2</sub>SnO<sub>4</sub> phase (with the highest intensity belonging to Zn<sub>2</sub>SnO<sub>4</sub>) are detected.

For the samples 2SZO-9SZO mixtures of SnO<sub>2</sub> and Zn<sub>2</sub>SnO<sub>4</sub> phases were obtained, while for the samples 11SZO-15SZO a mixture of ZnO and Zn<sub>2</sub>SnO<sub>4</sub> was observed. An interesting behavior was noticed for the samples 2SZO and 15SZO, namely, for the sample 2SZO (with 97.5 mol % SnO<sub>2</sub>) the diffraction lines assigned to Zn<sub>2</sub>SnO<sub>4</sub> have a lower intensity than those obtained for the 15SZO sample (2.5 mol% SnO<sub>2</sub>).

At 1400 and 1500 °C no changes of the phase composition of the samples thermally treated at 1300 °C were observed.

Table 1

Phase composition of the studied samples thermally treated at different temperatures

Samples	Initial composition (mol.%)		Phase composition			
	SnO <sub>2</sub>	ZnO	500°C	900°C	1000°C	1300°C
1 SZO	100.0	0	SnO <sub>2</sub>	SnO <sub>2</sub>	SnO <sub>2</sub>	SnO <sub>2</sub>
2 SZO	97.5	2.5	SnO <sub>2</sub> , ZnO	SnO <sub>2</sub> , ZnO	SnO <sub>2</sub> , Zn <sub>2</sub> SnO <sub>4</sub>	SnO <sub>2ss</sub> , Zn <sub>2</sub> SnO <sub>4</sub>
3 SZO	95.0	5.0	SnO <sub>2</sub> , ZnO	SnO <sub>2</sub> , ZnO	SnO <sub>2</sub> , Zn <sub>2</sub> SnO <sub>4</sub>	SnO <sub>2</sub> , Zn <sub>2</sub> SnO <sub>4</sub>
4 SZO	90.0	10.0	SnO <sub>2</sub> , ZnO	SnO <sub>2</sub> , Zn <sub>2</sub> SnO <sub>4</sub> , ZnO	SnO <sub>2</sub> , Zn <sub>2</sub> SnO <sub>4</sub>	SnO <sub>2</sub> , Zn <sub>2</sub> SnO <sub>4</sub>
5 SZO	80.0	20.0	SnO <sub>2</sub> , ZnO	SnO <sub>2</sub> , Zn <sub>2</sub> SnO <sub>4</sub> , ZnO	SnO <sub>2</sub> , Zn <sub>2</sub> SnO <sub>4</sub>	SnO <sub>2</sub> , Zn <sub>2</sub> SnO <sub>4</sub>

Table 1 (continued)

6 SZO	70.0	30.0	SnO <sub>2</sub> , ZnO	SnO <sub>2</sub> , Zn <sub>2</sub> SnO <sub>4</sub> , ZnO	SnO <sub>2</sub> , Zn <sub>2</sub> SnO <sub>4</sub>	SnO <sub>2</sub> , Zn <sub>2</sub> SnO <sub>4</sub>
7 SZO	60.0	40.0	SnO <sub>2</sub> , ZnO	SnO <sub>2</sub> , Zn <sub>2</sub> SnO <sub>4</sub> , ZnO	SnO <sub>2</sub> , Zn <sub>2</sub> SnO <sub>4</sub>	SnO <sub>2</sub> , Zn <sub>2</sub> SnO <sub>4</sub>
8 SZO	50.0	50.0	SnO <sub>2</sub> , ZnO	SnO <sub>2</sub> , Zn <sub>2</sub> SnO <sub>4</sub> , ZnO	SnO <sub>2</sub> , Zn <sub>2</sub> SnO <sub>4</sub>	SnO <sub>2</sub> , Zn <sub>2</sub> SnO <sub>4</sub>
9 SZO	40.0	60.0	SnO <sub>2</sub> , ZnO	SnO <sub>2</sub> , Zn <sub>2</sub> SnO <sub>4</sub> , ZnO	Zn <sub>2</sub> SnO <sub>4</sub> , SnO <sub>2</sub>	SnO <sub>2</sub> , Zn <sub>2</sub> SnO <sub>4</sub>
10 SZO	33.0	67.0	SnO <sub>2</sub> , ZnO	ZnO, Zn <sub>2</sub> SnO <sub>4</sub> , SnO <sub>2</sub>	Zn <sub>2</sub> SnO <sub>4</sub>	Zn <sub>2</sub> SnO <sub>4</sub>
11 SZO	30.0	70.0	ZnO, SnO <sub>2</sub>	ZnO, Zn <sub>2</sub> SnO <sub>4</sub> , SnO <sub>2</sub>	Zn <sub>2</sub> SnO <sub>4</sub> , ZnO	Zn <sub>2</sub> SnO <sub>4</sub> , ZnO
12 SZO	20.0	80.0	ZnO, SnO <sub>2</sub>	ZnO, Zn <sub>2</sub> SnO <sub>4</sub> , SnO <sub>2</sub>	Zn <sub>2</sub> SnO <sub>4</sub> , ZnO	Zn <sub>2</sub> SnO <sub>4</sub> , ZnO
13 SZO	10.0	90.0	ZnO, SnO <sub>2</sub>	ZnO, SnO <sub>2</sub>	Zn <sub>2</sub> SnO <sub>4</sub> , ZnO	Zn <sub>2</sub> SnO <sub>4</sub> , ZnO
14 SZO	5.0	95.0	ZnO, SnO <sub>2</sub>	ZnO, SnO <sub>2</sub>	Zn <sub>2</sub> SnO <sub>4</sub> , ZnO	ZnO, Zn <sub>2</sub> SnO <sub>4</sub>
15 SZO	2.5	97.5	ZnO, SnO <sub>2</sub>	ZnO, SnO <sub>2</sub>	Zn <sub>2</sub> SnO <sub>4</sub> , ZnO	ZnO, Zn <sub>2</sub> SnO <sub>4</sub>
16 SZO	0	100.0	ZnO	ZnO	ZnO	ZnO

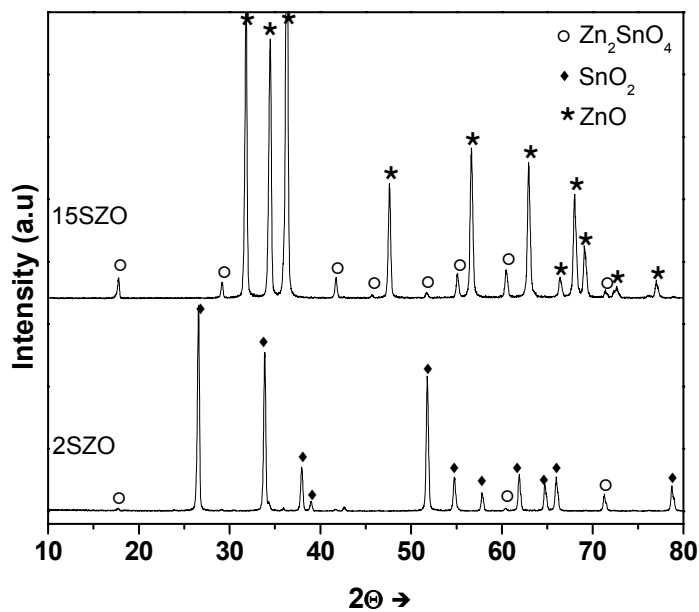


Fig. 3 – XRD patterns of the 2SZO and 15SZO thermally treated at 1300°C.

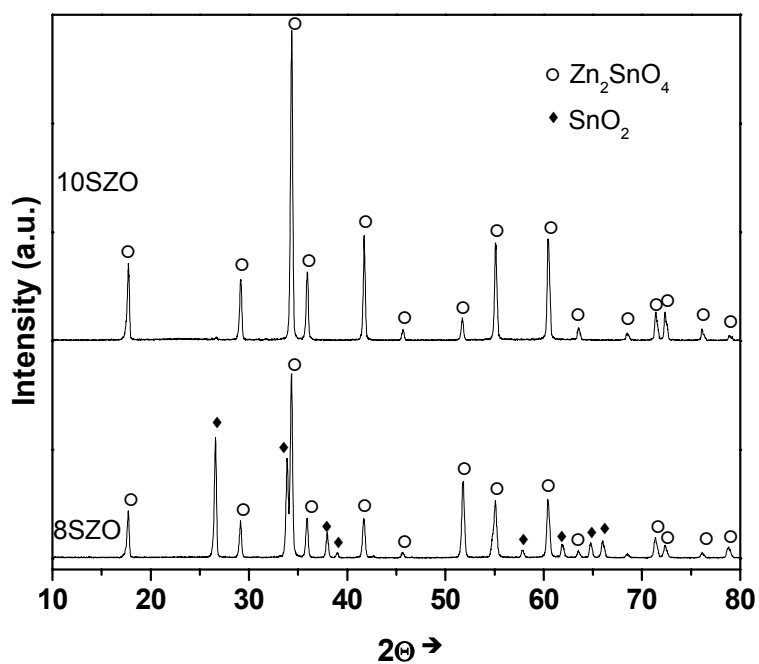


Fig. 4 – XRD patterns of the 8SZO and 10SZO thermally treated at 1300°C.

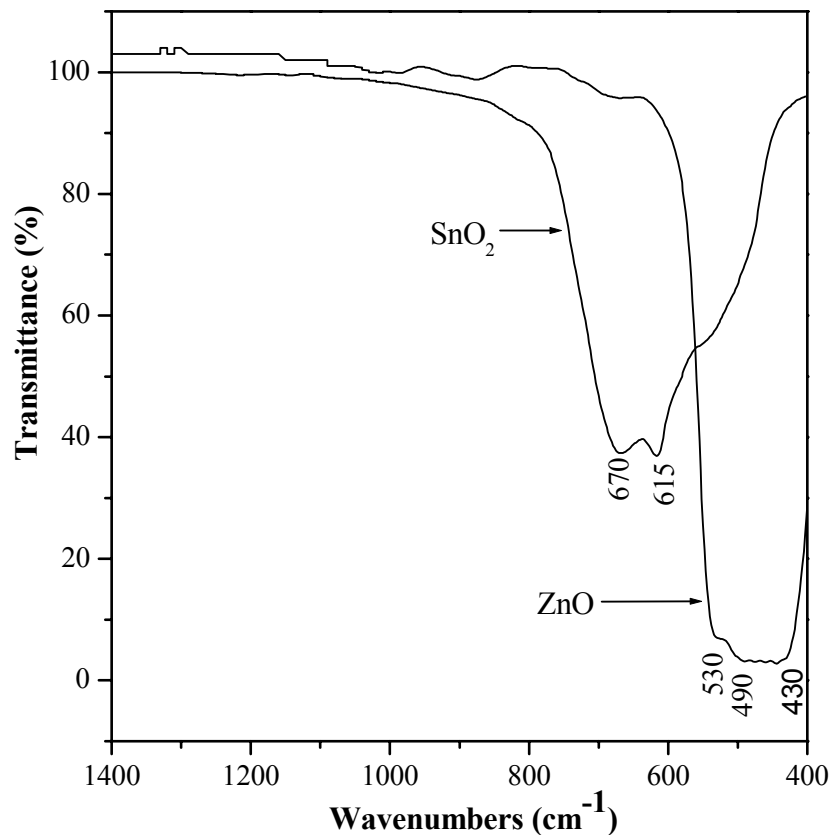


Fig. 5 – FT-IR spectra of the starting oxides.

The results obtained by XRD measurements were confirmed by FT-IR spectroscopy. The FT-IR spectra of the starting oxides (Fig. 5) show typical absorption bands of SnO<sub>2</sub><sup>18</sup> and ZnO<sup>19</sup> lattice.

The FT-IR spectra of the 8SZO sample, as-prepared and thermally treated at different temperatures are presented in Fig. 6. For 8SZO initial mixture the typical absorption bands of SnO<sub>2</sub> lattice at 667 and 616 cm<sup>-1</sup> and of ZnO lattice at 530, 495 and 440 cm<sup>-1</sup> were noticed. The 8SZO sample thermally treated at 600°C showed the existence of the same peaks for the SnO<sub>2</sub> lattice but the disappearance of the ZnO typical peaks. Relevant changes in the FT-IR spectrum of the sample thermally treated at 1000°C can be seen by the appearance of new absorption bands at 572 cm<sup>-1</sup> assigned to the Zn<sub>2</sub>SnO<sub>4</sub> spinel phase<sup>20</sup> and a shifting to smaller wave numbers of the vibration bands corresponding to Sn-O (655cm<sup>-1</sup>) and Zn-O (420 cm<sup>-1</sup>) bondings. The sample thermally treated over 1000°C exhibits the same FT-IR spectrum but

the decrease of the FT-IR bands intensity with increasing of temperature was found.

FT-IR spectra of the 2SZO, 8SZO, 10SZO and 15SZO samples thermally treated at 1300 °C with ten hours plateau are presented in Fig. 7. FT-IR spectrum of the 2SZO sample shows an abnormal transmission decrease and the disappearance of all typical bands belonging to SnO<sub>2</sub> (main phase identified by XRD). A similar behavior was previously observed in the case of SnO<sub>2</sub> based solid solution formation.<sup>21, 22</sup> For the 8SZO and 10SZO samples similar FT-IR vibration bands, but with different intensities, can be observed in good agreement with the XRD data that have shown the presence in these samples of the same spinel phase of zinc stannate.<sup>20</sup> Sample 15SZO keeps the shape and the position of the characteristic bands of ZnO, but the weak and broad absorption band placed at 650 cm<sup>-1</sup> might also be assigned to the Sn-O bonding.

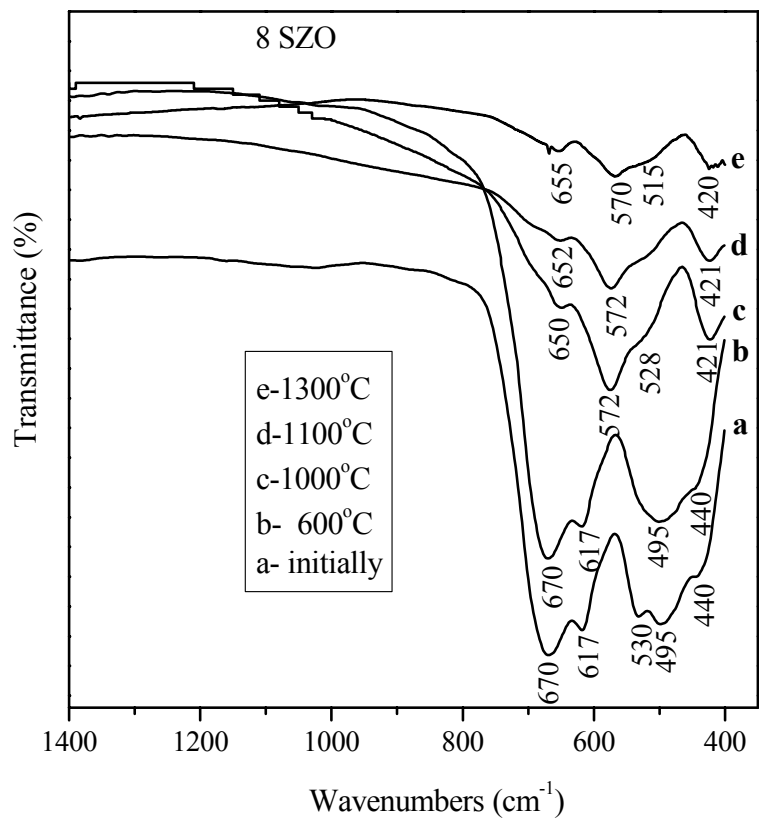


Fig. 6 – FT-IR spectra of the 8SZO sample thermally treated at different temperatures.

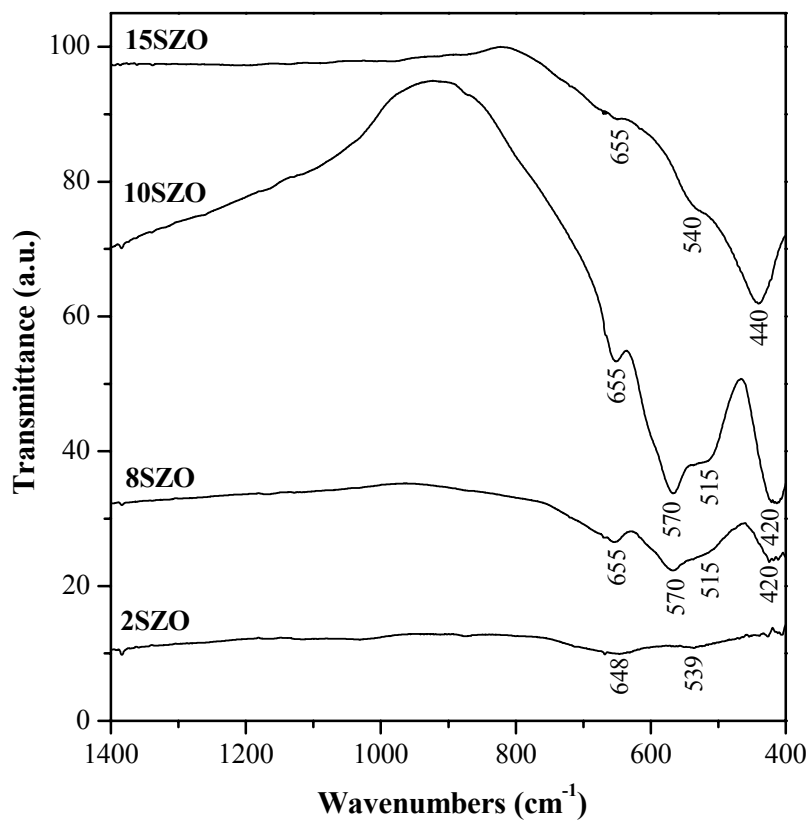
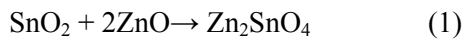


Fig. 7 – FT-IR spectra of selected samples thermally treated at 1300 °C, 10h.

## DISCUSSION

According to the results presented above the solid state reaction between SnO<sub>2</sub> and ZnO over the whole composition range and in the 500-1500 °C temperature interval leads to the formation of the only Zn<sub>2</sub>SnO<sub>4</sub> compound. The reaction of Zn<sub>2</sub>SnO<sub>4</sub> formation is the following:



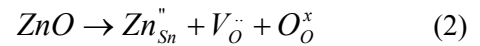
This compound was obtained even in non-isothermal condition (with the heating rate of 10°C/min) up to 1500 °C although DTA analysis doesn't indicate the presence of any definite thermal effect. It seems that the interaction between the two components takes place continuously. The Zn<sub>2</sub>SnO<sub>4</sub> compound was identified by XRD also in the 2SZO sample with 2.5 mol % ZnO, thermally treated starting with 1000°C.

It is well known that Zn<sub>2</sub>SnO<sub>4</sub> has an inverse cubic spinel structure. The unit cell is face-centered cubic (space group  $\text{Fd}\bar{3}\text{m}$  or  $\text{O}_h^7$ ) with lattice parameter  $a_0 = 8.65 \text{ \AA}$ .<sup>23</sup> The tetrahedral voids are occupied by Zn<sup>2+</sup> atoms and the octahedral voids are occupied randomly both by Zn<sup>2+</sup> and Sn<sup>4+</sup> atoms.<sup>24, 25</sup> It should be mentioned that Zn<sup>2+</sup> in tetrahedral coordination has ionic radius of 0.6 Å, but in octahedral coordination its ionic radius is 0.75 Å.<sup>26</sup> The ionic radius of Sn<sup>4+</sup> is 0.69 Å.<sup>22</sup> It should be mentioned that Sn<sup>4+</sup> in the SnO<sub>2</sub> rutile type structure adopts octahedral coordination while Zn<sup>2+</sup> from ZnO wurtzite type structure has a tetrahedral coordination. According to Rečnick *et al.*<sup>26</sup> the formation of octahedral sites in the ZnO lattice is favored by the clustering of Zn- vacancies at the ZnO surface at a temperature higher than 700°C. The octahedral sites located at the center of the vacancy clusters would be very favorable for Sn<sup>4+</sup> cations chemisorption and further interaction between the components.

In our experiments formation of the ZnSnO<sub>3</sub> compound was not emphasized although Zhang *et al.*<sup>15</sup> reported the obtaining of these compound at 1427 °C. From a general crystallographic point of view Kovacheva and Petrov<sup>14</sup> however showed that ZnSnO<sub>3</sub> cannot adopt a perovskite structure under normal conditions, since the ionic radius of Zn<sup>2+</sup> is too small. Inaguma *et al.*<sup>17</sup> pointed out that the solid-state reaction between ZnO and SnO<sub>2</sub> in the

pressure range from ambient pressure to 5 GPa gives neither LiNbO<sub>3</sub>(LN)-type ZnSnO<sub>3</sub> nor ilmenite (IL)-type ZnSnO<sub>3</sub>, resulting in a mixture of spinel-type Zn<sub>2</sub>SnO<sub>4</sub> and rutile-type SnO<sub>2</sub>. The authors also argue that the ilmenite structure is not the thermodynamically favored form at any pressure though the molar volumes of IL-type ZnSnO<sub>3</sub> (56.78 Å<sup>3</sup>) is smaller than that of (1/2 Zn<sub>2</sub>SnO<sub>4</sub> + 1/2 SnO<sub>2</sub>) (58.3 Å<sup>3</sup>) and greater than that of LN-type ZnSnO<sub>3</sub> (55.97 Å<sup>3</sup>).

Additional information on the phase formation was given by FT-IR Spectroscopy. Thus for the sample with starting composition of 97.5 mol % SnO<sub>2</sub> and 2.5 mol % ZnO (2SZO) thermally treated at 1300°C has shown in the FT-IR spectrum an abnormal reduction of transmission and the disappearance of the characteristic bands. Otherwise in XRD patterns characteristics lines corresponding to the Zn<sub>2</sub>SnO<sub>4</sub> have a very small intensity in comparison with the sample with starting composition of 97.5 mol % ZnO and 2.5 mol % SnO<sub>2</sub> (15SZO). Nevertheless appearance of FT-IR spectrum similar with those obtained in our previously experiments<sup>21, 22</sup> suggests a partially SnO<sub>2</sub> solid solution formation. The possible equations for substitution of Sn<sup>4+</sup> with Zn<sup>2+</sup> are given by Fayat and Castro<sup>27</sup> as following:



In this case, zinc ions could adopt octahedral coordination with ionic radius of 0.75 Å.

In Fig. 8 SEM image of the 2SZO is visualized.

Homogeneous surface phase was pointed out by SEM. The presence of SnO<sub>2</sub>ss solid solution could be assigned to lighter layer surrounding the grains. Further studies are necessary to clarify this aspect.

Based on the results discussed above, the subsolidus phase relations of SnO<sub>2</sub>-ZnO system show that the system is divided in two binary subsystems: SnO<sub>2</sub>-Zn<sub>2</sub>SnO<sub>4</sub> (0-66.6 mol% ZnO initial compositions) and Zn<sub>2</sub>SnO<sub>4</sub>-ZnO (66.6-100 mol% ZnO initial compositions).

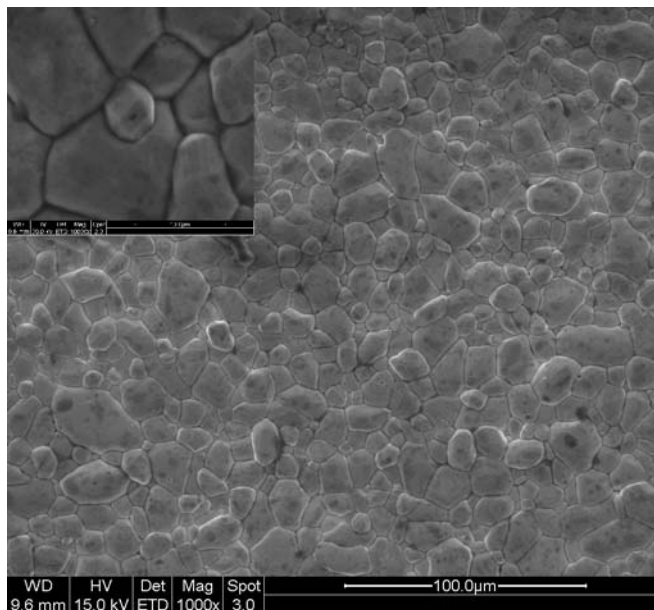


Fig. 8 – SEM image of 2SZO sample thermally treated.

## CONCLUSIONS

A systematic study of the phase formation over the whole compositional range of the ZnO-SnO<sub>2</sub> binary system in the 500-1500 °C temperature domain was approached.

Starting with 900 °C temperature the formation of the Zn<sub>2</sub>SnO<sub>4</sub> with inverse spinel type structure was emphasized in all samples.

The formation of the ZnSnO<sub>3</sub> was not observed in the experimental conditions used.

In the 1000-1500 °C temperature range no change in the phase composition was observed.

The presence of the Zn<sub>2</sub>SnO<sub>2</sub> compound divides the system in two subsolidus domains: SnO<sub>2</sub>-Zn<sub>2</sub>SnO<sub>4</sub> and Zn<sub>2</sub>SnO<sub>4</sub>-ZnO

FT-IR results confirm the XRD measurements and additionally suggest the limited solid solution formation in the region closed to pure SnO<sub>2</sub>.

## REFERENCES

1. P.R. Bueno, J. A.Varela and E. Longo, *J. Eur. Ceram. Soc.*, **2007**, 27, 4313.
2. K. Park, J.K. Seong, Y. Kwon, S. Nahm and W.-S.Cho, *Mat. Res.Bull.*, **2008**, 43, 54.
3. S. Major, S. Kumar, M. Bhatnagar and K.L. Chopra, *Appl.Phys.Lett.*, **1986**, 49, 394.
4. Gupta, T. K., *J. Mat. Res.*, **1992**, 12, 3280.
5. C.H. Kwon, M.N. Hong, D.H. Yun, K. Lee, S.T. Kim, Y.H. Roh and B.H. Lee, *Sens.Actuators*, **1995**, 24-25, 610.
6. M. Ihoș, F. Manea, G. Bocea and M. Jitaru, *Rev. Roum. Chim.*, **2009**, 54, 301.
7. A.M. Popescu, G. Nipan, S. Mihaiu, V. Constantin, M. Olteanu and N. Shumilkin, *Rev.Roum.Chim.*, **2010**, 55, 319.
8. C. Wang, X.M. Wang, B.Q. Xu, J.C. Zhao, B.X. Mai, P.A. Peng, G.Y. Sheng and J.M. Fu, *J. Photochem. Photobiol.A:Chem.*, **2004**, 168, 47.
9. A. Anastasiou, M.H.J. Lee, C. Leach and R. Freer, *J. Eur.Ceram.Soc.*, **2004**, 24, 1171.
10. T. Hashemi, H.M. Al-allak, J. Illingsworth, A.W. Brinkman and J.Woods, *J. Mater. Sci. Lett.*, **1990**, 7, 776.
11. F. Belliard, P.A. Connor and J.T.S. Irvine, *Solid State Ionics*, **2000**, 135, 163.
12. N. Nikolic, Z. Marinovic and T. Sreckovic, *J.Mat. Sci.*, **2004**, 39, 5239.
13. Y.S. Shen and T. Zhang, *Sens. Actuators B Chem.*, **1993**, 12, 5.
14. D. Kovacheva and K. Petrov, *Solid State Ionics*, **1998**, 109, 327.
15. G.Z.Zang, J.F.Wang, H.C.Chen, W.B.Su, W.X.Wang, P.Qi and C.M.Wang, *J. Mat.Sci.*, **2004**, 39, 3537.
16. H.Q. Chiang, J.F.Wager, R.L. Hoffman, J. Jeong and D.A.Keszler, *Appl. Phys.Lett.*, **2005**, 86, 013503.
17. Y.Inaguma, M.Yoshida and T.Katsumata, *J. Am. Chem. Soc.*, **2008**, 130, 6704.
18. E.N.Iurchenko and G.N. Kustova, „Kolebantie spectri neorganicheskih soedinenii”, Ed. Nauk, Novosibirsk, 1981.
19. M. Andrés-Vergés and C.J. Serna, *J. Mater. Sci. Lett.*, **1988**, 7, 970.
20. M. V. Nikolić, T. Ivetić, K. M. Paraskevopoulos, K. T. Zorbaz, V. Blagojević and D. Vasiljević-Radović, *J. Eur.Ceram.Soc.*, **2007**, 27, 3727.
21. S. Mihaiu, O. Scarlat, Gh. Aldica and M. Zaharescu, *J. Eur.Ceram.Soc.*, **2001**, 21, 1801.
22. S. Mihaiu, N. Dragan, O. Scarlat, A. Szatvanyi, D. Crisan and M. Zaharescu, *Rev. Roum. Chim.*, **2002**, 47, 843.
23. D. Segev and S.-H. Wei, *Phys. Rev. B*, **2005**, 71, 125.
24. W. Su-Huai and S.B. Zhang, *Phys. Rev. B*, **2001**, 63, 112.
25. R.D. Shannon and C.T. Prewitt, *Acta Cryst.*, **1969**, B25, 25.
26. A. Rečnik, N. Daneu and S. Bernik, *J. Eur.Ceram.Soc.*, **2007**, 27, 1998.
27. J. Fayat and M.S. Castro, *J. Eur.Ceram.Soc.*, **2003**, 23, 1585.



